Astrophys Space Sci (2007) 312: 103–111
DOI 10.1007/s10509-007-9658-6

ORIGINAL ARTICLE

Electron surfing acceleration by electrostatic waves in current sheet

De-Yu Wang · Quan-Ming Lu

Received: 25 January 2007 / Accepted: 23 August 2007 / Published online: 10 October 2007

Abstract The electron surfing acceleration in the current sheet with perpendicular propagating electrostatic waves is studied using analytical theories and test particle simulations. The trapped electron moving with the phase velocity v_p of wave may be accelerated effectively in the outflow direction by $\frac{ev_p}{c} \times B_z$ force until the electron is de-trapped from the wave potential. A criterion $K > 0$ for the electron surfing acceleration is obtained. The electron will escape from the boundary of current sheet quickly, if this criterion does not hold. The maximum velocity of surfing acceleration is about the same as the electric drift velocity. Superposed longitudinal magnetic field along the wave propagation is favorable for the electron surfing acceleration in the current sheet.

Keywords Particle acceleration · Electrostatic wave · Current sheet

PACS 96.50.Pw · 94.20.Rr

1 Introduction

Magnetic reconnection can lead to a fast energy conversion from electromagnetic fields to particles, it occurs in many space and astrophysical plasma systems. However, magnetic reconnection cannot take place in an ideal magnetohydrodynamics (MHD) plasma, because the magnetic field is frozen in an ideal MHD plasma. The DC electric field produced during the non-ideal MHD magnetic reconnection can directly accelerate charged particles. Speiser (1965) was the first one who study the details of particle dynamics in the tail current sheet with a uniform normal magnetic field, and then the test particle simulation is accepted (Zhu and Parks 1993; Browning and Vekstein 2001; Himilton et al. 2003), the particles are found to be accelerated by the electric field in the current sheet with a longitudinal magnetic field. Litvinenko and Somov (1993) obtained an analytical solution to describe such electric field acceleration processes.

Recently, Horiuchi and Sato (1999) performed three-dimensional particle simulations to study collisionless reconnection and found that the lower hybrid drift instability is excited in the early stage of collisionless reconnection around $\omega_{ce}t = 510$ (ω_{ce} is the electron cyclotron frequency). These excited lower hybrid drift waves are electrostatic waves propagating along the direction perpendicular to the reconnection plane. With three-dimensional particle simulations (Drake et al. 2003) also found that the electrostatic waves can be excited in the early stage of magnetic reconnection around the $\omega_{ci}t = 0.55$ by Buneman instability, where ω_{ci} is the ion cyclotron frequency, and these waves propagate in the direction perpendicular to reconnection plane. Therefore, plasma instabilities not only give rise anomalous resistivity, but also amplify various plasma waves during the magnetic reconnection. These waves have been characterized in magnetic reconnections in the magnetotail (Farrell et al. 2002; Øieroset et al. 2002) and near Earth's dayside magnetopause (Labelle and Treumann 1988; Bale et al. 2002). A magnetic reconnection event in the tail of interplanetary magnetic cloud were analyzed with

D.-Y. Wang (✉)
Purple Mountain Observatory, Chinese Academy of Sciences, Nanjing 210008, China
e-mail: d_y_wang@pmo.ac.cn

Q.-M. Lu
School of Earth and Space Sciences, University of Science and Technology of China, Hefei 230026, China
e-mail: qmlu@ustc.edu.cn

Wind spacecraft data (Zhong et al. 2005). It is found that the electrons are accelerated, and the plasma waves activity enhanced near electron plasma frequency f_{pe} and $2f_{pe}$ during the reconnection, simultaneously. These events give observational evidences for electron acceleration in the magnetic reconnection, which are possible to be correlated with plasma waves.

An important unresolved problem is that besides the particles are accelerated directly by DC electric field, whether these excited electrostatic and electromagnetic waves have influence on the particle acceleration during magnetic reconnection? In fact, the electron acceleration in an electrostatic wave was studied in laser plasma (Dawson et al. 1983; Sugihara et al. 1984). They considered that electrons can be trapped by electrostatic waves. The trapped electrons moving with phase velocity v_p of wave see an inductive electric field $\frac{v_p}{c} \times B_z$, if an uniform transverse magnetic field B_z perpendicular to wave vector is superposed. This magnetic field deflects electrons across the electrostatic wave fronts, thus preventing them from outrunning the wave potential, which like surfers cutting across the face of an ocean wave. Therefore, these trapped electrons may be accelerated continuously by $\frac{ev_p}{c} \times B_z$ force. Sometimes, this acceleration is called surfing acceleration, or surfatron (Katsouleas and Dawson 1983). In this paper, similar to the electron acceleration by DC electric field in the current sheet (Speiser 1965; Zhu and Parks 1993; Litvinenko and Somov 1993), we present a model of electron movement in the current sheet under the interaction of the shear magnetic field and the perpendicular propagating electrostatic waves.

The paper is organized as follows. The zeroth and first order analytical solution of the electron surfing acceleration trajectory are studied in Sect. 2. The test particle simulations for electron movement are described in Sect. 3. We discuss and summarize our results in Sect. 4.

2 Theoretical model and its analytical solution

It is assumed that the current sheet with magnetic shear lie in the x–z plane of a Cartesian coordinate system, the magnetic fields and electrostatic wave inside the sheet are written as follows:

$$\mathbf{B} = \left(\frac{z}{d}B_0, B_y, B_z\right), \tag{1}$$

$$\mathbf{E} = (0, E_y, 0) \tag{2}$$

where B_0, B_y, B_z are constant. $B_x = \frac{z}{d}B_0$ is the shear magnetic field component; B_y and B_z are longitudinal and transverse magnetic field components, respectively. The d is the half thickness of the current sheet, as shown in Fig. 1. In fact, both transverse and longitudinal components of magnetic field vary with time and space during the magnetic reconnection, even if in the steady reconnection. As an approximation for the charged particle surfing acceleration in current sheet, these magnetic field components are assumed to be invariant in time and space, and the effects of electrons on the electromagnetic field are neglected. These expressions are first nonzero terms of Taylor expansion near the plane $z = 0$ during magnetic reconnection. $E_y = E_0 \sin(ky - \Omega t)$ is an electrostatic wave, it is assumed that this wave is propagating with phase velocity v_p along the y axis direction. E_0, Ω and k are amplitude, frequency and wave number of electrostatic wave, respectively.

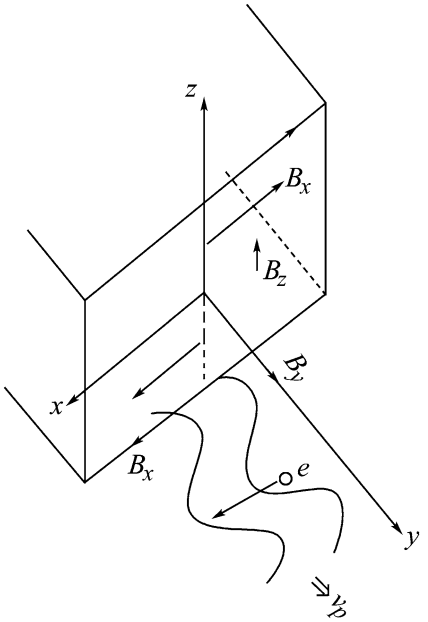

Fig. 1 Sketch of the perpendicular propagating electrostatic wave in current sheet

The non-relativistic motion equation for an electron can be expressed as

$$m\frac{d\mathbf{v}}{dt} = -e\left(\mathbf{E}_y + \frac{1}{c}\mathbf{v} \times \mathbf{B}\right) \tag{3}$$

where e is unit charge and m is mass of electron. It is convenient to use a wave frame coordinate system (X, Y, Z) to describe the electron moving in an electrostatic wave field. In this case, $X = x$, $Y = y - v_p t$, $Z = z$, and $v_y = V_Y + v_p$, where $v_p = \frac{\Omega}{k}$ is phase velocity of wave, and V_Y is the Y component of electron oscillation velocity in the wave frame coordinate system. For simplicity, it is assumed that E_0 and v_p maintain constant in the current sheet. Insertion of the electrostatic wave field and the shear magnetic field into (3) in the wave frame coordinate system, it yields.

$$\frac{dv_x}{dt} = -(V_Y + v_p)\omega_\perp + v_z\omega_\parallel, \tag{4}$$

$$\frac{dV_Y}{dt} = -\frac{e}{m}E_y + v_x\omega_\perp - v_z\frac{z}{d}\omega_0, \tag{5}$$

$$\frac{dv_z}{dt} = -v_x\omega_\parallel + (V_Y + v_p)\frac{z}{d}\omega_0 \tag{6}$$

where $\omega_0 = \frac{eB_0}{mc}$, $\omega_\perp = \frac{eB_z}{mc}$ and $\omega_\parallel = \frac{eB_y}{mc}$ are electron cyclotron frequency of magnetic field B_0, B_z, B_y, respectively. We assume that the electron is initially deeply trapped by the potential of electrostatic wave E_y moving with phase velocity v_p. The trapped electron in current sheet interacts with inductive electric fields $\frac{v_p}{c} \times B_z$ and $\frac{v_p}{c}\frac{z}{d} \times B_0$ from the Lorentz transformation, as described in (4–6).

2.1 Zeroth order analytical solution

In the following discussion, the relation $|V_Y| \ll |v_p|$ is usually assumed to hold within the trapping. In this case, we take

$$\begin{aligned} v_x &= v_{x0} + v_{x1} + \text{——}, \\ V_Y &= V_{Y0} + V_{Y1} + \text{——}, \\ v_z &= v_{z0} + v_{z1} + \text{——}. \end{aligned} \tag{7}$$

For the zeroth order approximation, V_{Y0} can be negligible in (4) and (6). Thus

$$\frac{dv_{x0}}{dt} = -v_p\omega_\perp + v_{z0}\omega_\parallel, \tag{8}$$

$$\frac{dV_{Y0}}{dt} = -\frac{eE_0}{m}\sin(kY_0) + v_{x0}\omega_\perp - v_{z0}\frac{z_0}{d}\omega_0, \tag{9}$$

$$\frac{dv_{z0}}{dt} = -v_{x0}\omega_\parallel + v_p\frac{z_0}{d}\omega_0. \tag{10}$$

The v_{x0} can be expressed as

$$v_{x0} - v_{x0}(0) = -v_p\omega_\perp t + (z_0 - z_0(0))\omega_\parallel \tag{11}$$

where $z_0(0)$ and $v_{x0}(0)$ are the initial value of z_0 and v_{x0}, respectively. Insertion of (8) into the derivative of (10), it gives

$$\frac{d^2v_{z0}}{dt^2} \pm Q^2 v_{z0} = \omega_\parallel\omega_\perp v_p \tag{12}$$

where $Q^2 = |K|$ and

$$K = \omega_\parallel^2 - \frac{v_p}{d}\omega_0. \tag{13}$$

The plus sign in (12) corresponds to $K > 0$, and the minus sign corresponds to $K < 0$. Equation (12) describes a cosinoidal oscillation equation of v_{z0} for $K > 0$. Under the initial condition, $v_{z0}(0) = 0$, the solution of (12) may be expressed as

$$v_{z0} = \begin{cases} A_E(1 - \cos Qt) & \text{for } K > 0, \\ -A_E(1 - \cosh Qt) & \text{for } K < 0 \end{cases} \tag{14}$$

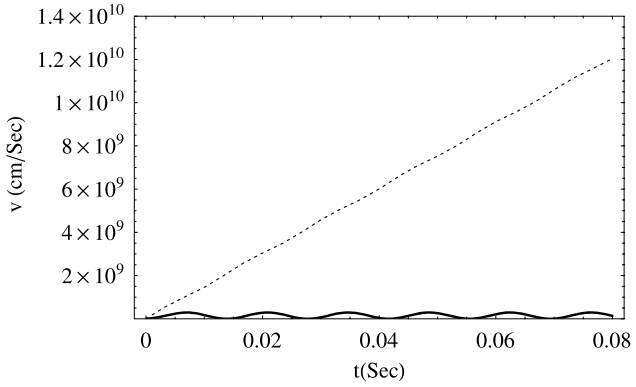

Fig. 2 The time evolution of electron velocity trajectory for the zeroth order analytical solution of v_{x0} (*dot line*) and v_{z0} (*solid line*) with the parameters shown in Table 1, $K > 0$

where $A_E = \frac{\omega_\perp\omega_\parallel v_p}{Q^2}$ is the amplitude of v_{z0}. Integration of (14), we obtain

$$z_0 - z_0(0) = \begin{cases} A_E t\left[1 - \frac{1}{Qt}\sin Qt\right] & \text{for } K > 0, \\ -A_E t\left[1 - \frac{1}{Qt}\sinh Qt\right] & \text{for } K < 0. \end{cases} \tag{15}$$

Insertion of (15) into (11), we obtain

$$v_{x0} - v_{x0}(0) = \begin{cases} -\omega_\perp v_p t\left[1 - \frac{\omega_\parallel^2}{Q^2}\left(1 - \frac{1}{Qt}\sin Qt\right)\right] & \text{for } K > 0, \\ -\omega_\perp v_p t\left[1 + \frac{\omega_\parallel^2}{Q^2}\left(1 - \frac{1}{Qt}\sinh Qt\right)\right] & \text{for } K < 0. \end{cases} \tag{16}$$

The trajectory of the zeroth order electron velocity v_{x0} and v_{z0} have been calculated for different parameters of current sheet, as shown in Fig. 2 and Fig. 3. The parameters of these figures are given in the Table 1. Figure 2 is an examples for the cases of $K > 0$. Figure 3 is another example for the case of $K < 0$. It is readily found from these figures that the electron acceleration is wholly different for the cases of $K > 0$ and $K < 0$. In the case of $K > 0$, the electron can be accelerated mainly by $\frac{ev_p}{c} \times B_z$ force in the current sheet plane (x, z), and the velocity value of v_{x0} is often much larger than the value of $|v_{z0}|$. In the case of $K < 0$, on the other hand, the electron can be rapidly accelerated in the z direction, these electrons will escape rapidly from the z boundary of current sheet, and then the electron surfing acceleration process will stop. Meanwhile, the $v_{x0} < 0$ in the beginning stage of acceleration, as shown in Fig. 3, it means that the electron will be decelerated in the beginning stage in the case of $K < 0$. Therefore, we come to the conclusion that the $K > 0$ is a criterion for electrons can be effectively accelerated in the current sheet by surfing acceleration processes. This criterion does not exist in the electron surfing acceleration of laser plasma. It is also identified by the test particle simulation, as shown in Sect. 3.

Table 1 The calculation parameters for Figs. 2 and 3

Figure	ω_0 (1/s)	$\omega_\perp$ (1/s)	$\omega_\parallel$ (1/s)	v_p (cm/s)	d (cm)	K	B_z/B_0
2	1.76×10^3	1.76×10^2	-1.76×10^2	-10^9	10^7	>0	0.1
3	3.5×10^3	3.5×10^2	4.5×10^2	1.2×10^9	2×10^7	<0	0.1

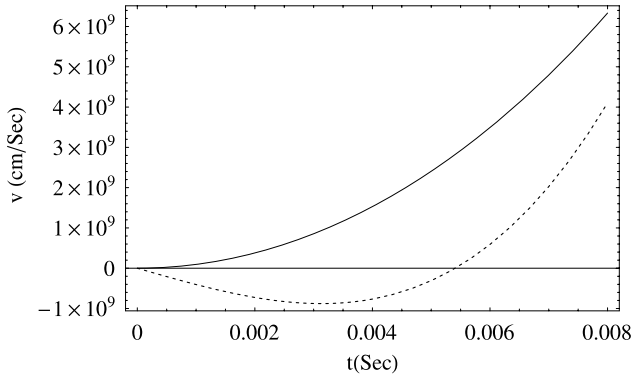

Fig. 3 The time evolution of electron velocity trajectory for the zeroth order analytical solution of v_{x0} (*dot line*) and v_{z0} (*solid line*) with the parameters shown in Table 1, $K<0$

Considering that v_{x0}, v_{z0} and z_0 in (9) are a known function of time. Derivation of (9), we obtain

$$\frac{d^2V_{Y0}}{dt^2}+R^2V_{Y0} = P_1+P_3\cos Qt-P_2\cos 2Qt-P_2Qt\sin Qt \qquad (17)$$

where $P_1=-\omega_\perp^2 v_p(1-\frac{\omega_\parallel^2}{Q^2})-P_2$, $P_2=A_E^2\frac{\omega_0}{d}$, $P_3=2P_2-\omega_\perp^2 v_p\frac{\omega_\parallel^2}{Q^2}$ and $R^2=\frac{ek}{m}E_0\cos(kY_0)$. We take approximation $R^2\simeq R_0^2=\frac{ek}{m}E_0$, when condition $kY_0\ll1$ holds. R_0^2 is independent of time, so that V_{Y0} can be solved analytically from (17) as

$$V_{Y0}-V_{Y0}(0)=C_1(1-\cos R_0t)+C_2(1-\cos Qt)+C_3Qt\sin Qt+C_4(1-\cos 2Qt) \qquad (18)$$

where $C_1=\frac{P_1}{R_0^2}-C_2-C_4$, $C_2=\frac{P_3-2Q^2C_3}{Q^2-R_0^2}$, $C_3=\frac{P_2}{Q^2-R_0^2}$, $C_4=-\frac{P_2}{4Q^2-R_0^2}$ are independent of time. $V_{Y0}(0)$ is the initial condition of V_{Y0}. Figure 4(a) describes the time evolution of V_{Y0} for different E_0, but same B_y. Figure 4(b) describes the time evolution of V_{Y0} for different B_y, but same E_0, other parameters of Figs. 4(a) and (b) are the same as that in Fig. 2. It is found from these figures that the condition $|V_{Y0}|\ll|v_p|$ is only satisfied for the early stage of evolution time, but $|V_{Y0}|$ grows with the evolution time up to $|V_{Y0}|\geq|v_p|$. Anyway, we find from Figs. 4(a) and (b) that the condition $|V_{Y0}|\ll|v_p|$ can be satisfied for the longer evolution time, if the electrons interact with a large enough electrostatic wave, or a large enough longitudinal magnetic field B_y.

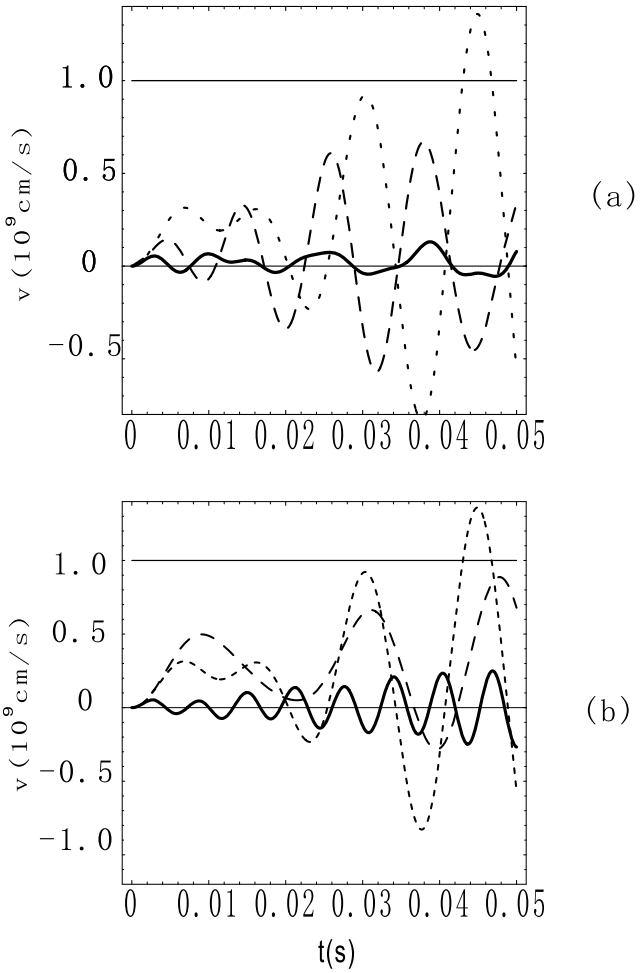

Fig. 4 The time evolution of electron velocity trajectory for the zeroth order analytical solution v_{Y0}. **a** Same $B_y=-10^{-5}$ G and different E_0. In the figure, the dot, dash and thick solid lines represent that case for $E_0=40$, 80, 320 mV/m, respectively. **b** Same $E_0=40$ mV/m and different B_y. In the figure, the dot, dash and thick solid lines represent that case for $B_y=-(0.5,1.0,5.0)\times10^{-5}$ G, respectively, and $v=-v_p$ (*thin solid line*). Other parameters are the same as that in Fig. 2

2.2 First order analytical solution

In the following section, we will only discuss the first order analytical solution for the case of $K>0$. Insertion of (7)

into (4), (5) and (6), we obtain the first order equations :

$$\frac{dv_{x1}}{dt} = -V_{Y0}\omega_\perp + v_{z1}\omega_\parallel, \tag{19}$$

$$\frac{dV_{Y1}}{dt} \simeq -\frac{eE_0}{m}\sin(kY_1) + v_{x1}\omega_\perp - v_{z1}\frac{z_0}{d}\omega_0 - v_{z0}\frac{z_1}{d}\omega_0, \tag{20}$$

$$\frac{dv_{z1}}{dt} = -v_{x1}\omega_\parallel + V_{Y0}\frac{z_0}{d}\omega_0 + v_p\frac{z_1}{d}\omega_0. \tag{21}$$

From (19) and (21), the first order analytical solution of v_{z1} can be expressed as

$$\begin{aligned} v_{z1} - v_{z1}(0) &= D_1(1-\cos R_0 t) + D_2(1-\cos Qt) \\ &\quad + D_3(1-\cos 2Qt) + D_4(1-\cos 3Qt) \\ &\quad + D_5(1-\cos(Q+R_0)t) + D_6(1-\cos(Q-R_0)t) \\ &\quad + D_7 Qt\sin Qt + D_8 2Qt\sin 2Qt \\ &\quad + D_9(Qt)^2\cos Qt + D_{10}R_0 t\sin R_0 t \end{aligned} \tag{22}$$

with

$$\begin{aligned} D_1 &= -\frac{C_1H_1 + 2R_0^2D_{10}}{Q^2 - R_0^2}; \\ D_2 &= \frac{(C_1+C_2+C_4)H_1 - 0.5C_3H_2}{Q^2} - D_1 - D_3 - D_4 - D_5 - D_6; \\ D_3 &= \frac{-C_4H_1 + (C_2+0.5C_3)H_2 - 8D_8Q^2}{3Q^2}; \\ D_4 &= \frac{3C_4H_2}{16Q^2}; \qquad D_5 = \frac{(1+\frac{R_0}{Q})C_1H_2}{2[(Q+R_0)^2 - Q^2]}; \\ D_6 &= \frac{(1-\frac{R_0}{Q})C_1H_2}{2[(Q-R_0)^2 - Q^2]}; \\ D_7 &= -\frac{2D_9Q^2 + C_2H_1 + (C_1+C_2+1.5C_4)H_2}{2Q^2}; \\ D_8 &= -\frac{(C_4 - 0.5C_3)H_2}{3Q^2}; \\ D_9 &= -\frac{C_3(H_1+H_2) + H_2C_2}{4Q^2}; \qquad D_{10} = \frac{C_1H_2}{Q^2 - R_0^2} \end{aligned} \tag{23}$$

where $H_1 = \omega_\parallel\omega_\perp\frac{\omega_\parallel^2}{Q^2}$ and $H_2 = A_E\frac{\omega_0}{d}$. D_i are independent of time. It is convenient to take the initial condition $v_{z1}(0) = 0$. Integration of (19), the first order analytical solution of v_{x1} can be expressed as

$$\begin{aligned} v_{x1} - v_{x1}(0) &= -\Big[C_1t\Big(1 - \frac{1}{R_0t}\sin R_0t\Big) + C_2t\Big(1 - \frac{1}{Qt}\sin Qt\Big) \\ &\quad + C_3\frac{1}{Q}(\sin Qt - Qt\cos Qt) \\ &\quad + C_4t\Big(1 - \frac{1}{2Qt}\sin 2Qt\Big)\Big]\omega_\perp \\ &\quad + \Big[D_1t\Big(1 - \frac{1}{R_0t}\sin R_0t\Big) + D_2t\Big(1 - \frac{1}{Qt}\sin Qt\Big) \\ &\quad + D_3t\Big(1 - \frac{1}{2Qt}\sin 2Qt\Big) + D_4t\Big(1 - \frac{1}{3Qt}\sin 3Qt\Big) \\ &\quad + D_5t\Big(1 - \frac{1}{(Q+R_0)t}\sin(Q+R_0)t\Big) \\ &\quad + D_6t\Big(1 - \frac{1}{(Q-R_0)t}\sin(Q-R_0)t\Big) \\ &\quad + D_7\frac{1}{Q}(\sin Qt - Qt\cos Qt) \\ &\quad + D_8\frac{1}{2Q}(\sin 2Qt - 2Qt\cos 2Qt) \\ &\quad + D_9\frac{1}{Q}(2Qt\cos Qt - (Q^2t^2 - 2)\sin Qt) \\ &\quad + D_{10}\frac{1}{R_0}(\sin R_0t - R_0t\cos R_0t)\Big]\omega_\parallel. \end{aligned} \tag{24}$$

The time evolution of electron velocity $v_{xt} = v_{x0} + v_{x1}$ and $v_{zt} = v_{z0} + v_{z1}$ have been calculated in Fig. 5(a) and Fig. 5(b) for two different E_0, respectively. The trajectory of electron velocity v_{x0} and v_{z0} are also displayed in these figures for comparison. It is readily found that the condition of first order electron velocity $v_{x1} \ll v_{x0}$ is usually satisfied for the early stage of evolution time.

3 Test particle simulation

The analytical model of electron surfing acceleration by $\frac{ev_p}{c} \times B_z$ force can only be established under the condition of $|v_Y| \ll |v_p|$ holds. Unfortunately, this condition is seldom satisfied during the later stage of time evolution, as discussed in above section. In this section, we describe the results of test particle simulation, where this condition is not assumed. In the calculation, the topology of electromagnetic fields are given by (1) and (2). The electron moves in such fixed electromagnetic fields, but the effects of the electrons on the electromagnetic fields are neglected. The electron dynamics is described by (3), and this equation is solved by means of the Boris algorithm (Birdsall and Langdonm 1985) with time step $\Delta t = 0.02\omega_0^{-1}$. Initially, the

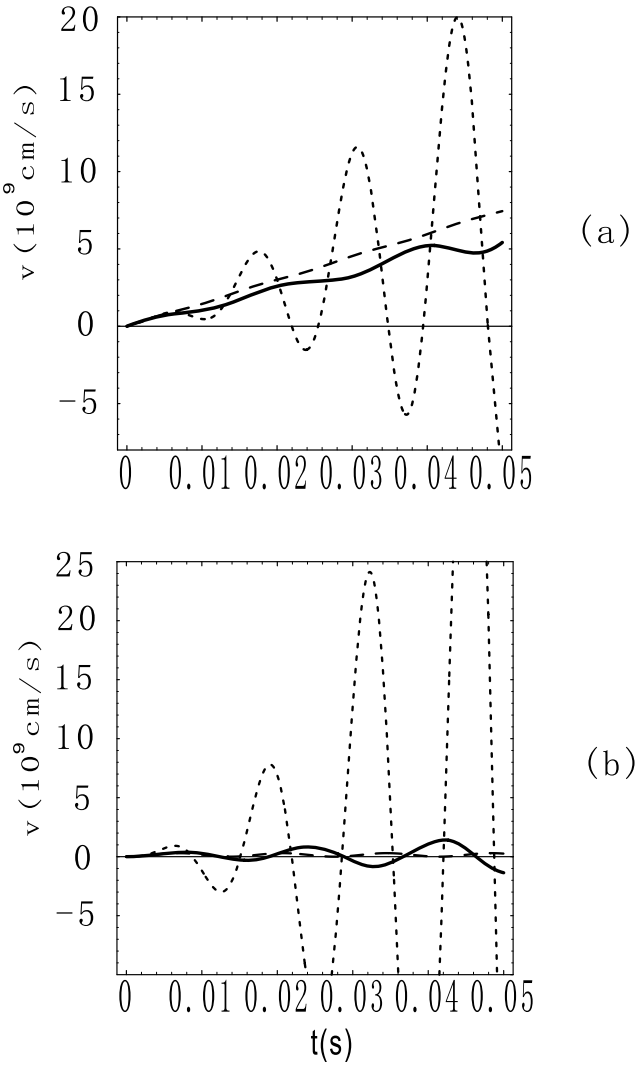

Fig. 5 The time evolution of electron velocity trajectory for the analytical solution **a** v_{x0} (*dash line*) and $v_{xt} = v_{x0} + v_{x1}$; **b** v_{z0} (*dash line*) and $v_{zt} = v_{z0} + v_{z1}$ with different $E_0 = 80$ mV/m (*dot line*), 40 mV/m (*solid line*), respectively. Other parameters are the same as that in Fig. 2

electron is at the point $(x, y, z) = (0, 0, 0)$ and its velocity is $(v_x, v_y, v_z) = (0, 0, 0)$.

Figure 6 describes the results for test particle simulation of the electron velocity in the case of $K < 0$. The parameters used in Fig. 6 are the same as that in Fig. 3. we can find from this figure that the electron will be fast accelerated in the z direction of current sheet plane for the case of $K < 0$, and then the electron escapes rapidly from the z boundary of current sheet, as it was discussed in above section and shown in Fig. 3.

Figures from Fig. 7 to Fig. 9 are three figures for the case of $K > 0$. Figure 7 makes a comparison between the v_x calculation results of the zeroth, first order analytical solution and test particle simulation. The parameters used in Fig. 7 are the same as that in Fig. 2, and the amplitude of electrostatic wave $E_0 = 50$ mV/m. It is found that the zeroth and first order analytical solution are consistent rather well with the test particle simulation in the early stage of time evolution. We think that it is also an indirect evidence that (4–6) in the wave frame are equal to (3) in the laboratory frame. However, these calculation results are inconsistent in the later stage of time evolution, which will be discussed in the following paragraph.

Figure 8 describes the results of time evolution of electron velocity trajectory for different amplitude of electrostatic wave E_0 and same longitudinal magnetic field. It is worthy of note from Figs. 7, 8(a) and 9 that a growing surfing acceleration velocity curve of v_x often turn into a horizontal oscillation curve at turning point S. That means that the test electron de-traps from the potential of electrostatic waves at this point, and then the electron cannot be accelerated continuously in the current sheet plane by $\frac{ev_p}{c} \times B_z$ force after this point. The turning point S does not display in the analytical solution because the approximation condition of $|V_{Y0}| \ll |v_p|$ does not hold at this point. We find from Fig. 8(a) that the v_x velocity value at the turning point S increases with the increasing of E_0, so that the electron can be accelerated up to higher energy when it interacts with a stronger electrostatic wave. On the other hand, the electron will be de-trapped easily from the potential of a weak electrostatic wave, as shown in the solid line of Fig. 8(a). It is found from Fig. 8(b) that the velocity of accelerated electron v_x is usually much larger than v_z for the case of $K > 0$ in the same way as that in Fig. 2 and Fig. 5.

Figure 9 describes the time evolution of electron velocity for different B_y and same E_0. It is readily to find that the longitudinal magnetic field B_y also play an important role in the electron surfing acceleration in current sheet. The electron acceleration velocity has a larger turning point, when a stronger B_y is superposed, as shown in the dot line and dish line of Fig. 9. The observations of Øieroset et al. (2002) found that the longitudinal magnetic field B_y at magnetotail may be rather large up to $B_y \sim 0.5B_0$ (Pritchett 2006).

4 Discussions and summary

It was assumed in above section that the electron was trapped within the electrostatic wave potential during the surfing acceleration processes. The criterion for the trapped electron can be estimated by examining the Y component of the force on the electron in the wave frame

$$F_Y = -\frac{e}{m}E_0 \sin kY + v_x\omega_\perp - v_z\frac{z}{d}\omega_0. \tag{25}$$

The first term in the right hand of (25) is the trapping term, the second and third terms are the de-trapping term. For small oscillation case, we can use approximation $F_Y \simeq 0$ in the left hand of (25), and the zeroth order analytical solution

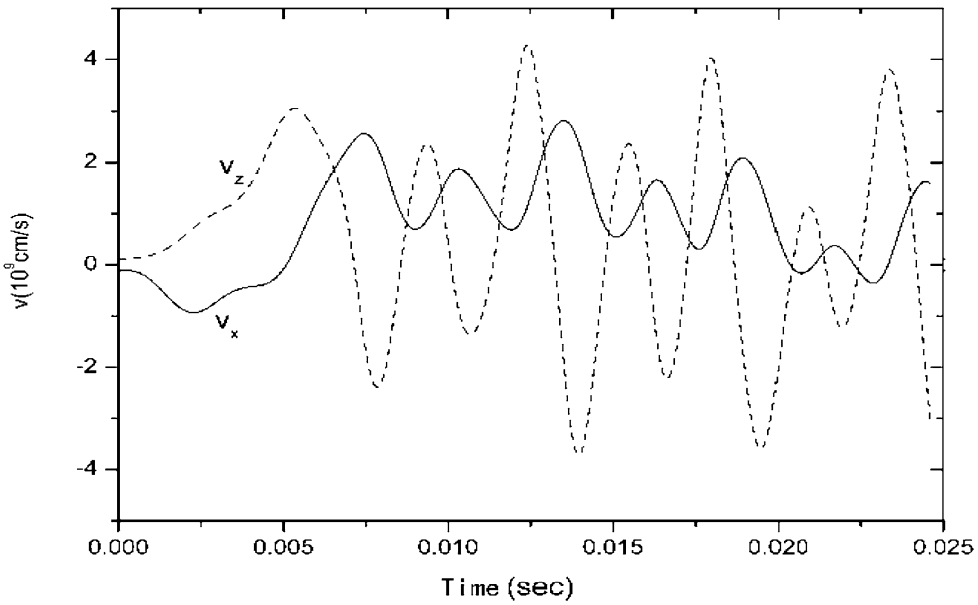

Fig. 6 The time evolution of electron velocity v_x and v_z trajectory by test particle simulation for $K < 0$ with $E_0 = 80$ mV/m. Other parameters are the same as that in Fig. 3

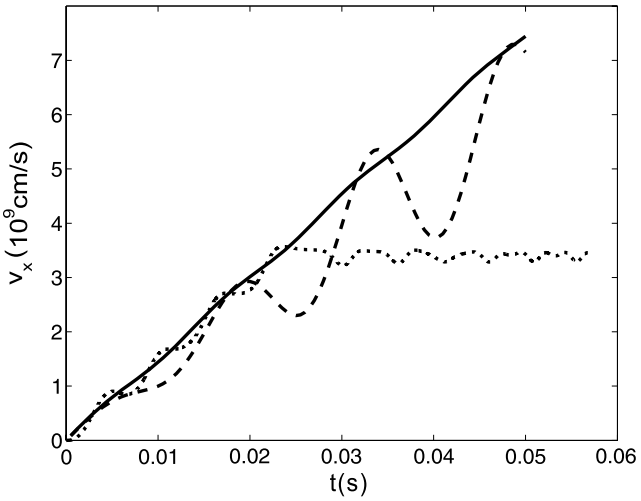

Fig. 7 Comparison of the time evolution of electron velocity trajectory between analytical solution and test particle simulation with same $E_0 = 50$ mV/m. Other parameters are the same as that in Fig. 2. In the figure, the solid, dash and dot lines represent that case for the zeroth order analytical solution v_{x0}, amount of the zeroth and first order analytical solution $v_{xt} = v_{x0} + v_{x1}$ and test particle simulation, respectively

v_{x0}, v_{z0}, z_0 instead of v_x, v_z, z in the right hand of (25). In the case of longitudinal magnetic field $B_y \to 0$, it is found $v_{z0} \to 0$ from (14), so that the third term in (25) approaches to zero. Hence, if the relation

$$v_{x0} \le V_E = \frac{E_0 c}{B_z} \tag{26}$$

holds, the initial trapped electron never de-traps from wave potential. It is worth noting that the V_E is the $\mathbf{E_0} \times \mathbf{B_z}$ electric drift velocity (Dawson et al. 1983). We find that V_E value of (26) is about the same as the v_x value at the turning point S from test particle simulation, as shown in Fig. 8(a). In the condition of $E_0 = 80$ mV/m and other parameters are the same as that in Fig. 2, the maximum velocity of electron surfing acceleration is about 20 keV. In consideration of $v_{x0} \simeq \frac{\omega_\perp \omega_0 v_p^2 t}{dQ^2}$ from (16), the acceleration limitation time of electron de-trapping t_d can be expressed as

$$t_d \le \frac{eE_0 Q^2 d}{m\omega_\perp^2 \omega_0 v_p^2}. \tag{27}$$

It is proportional to the amplitude of electrostatic wave E_0. The value t_d is also about the same as the time at turning point S. Otherwise, it also explain qualitatively that the stronger amplitude of electrostatic waves E_0 corresponds to the larger de-trapping velocity v_x, as shown in Fig. 8(a).

In the case of $B_y \neq 0$, it is found that $v_{x0}\omega_\perp$ often has the same sign as $v_{z0}\frac{z_0}{d}\omega_0$, so that the second and the third term cancel each other in the right hand of (25). Using (14), (15) and (16), we obtain

$$v_{x0}\omega_\perp - v_{z0}\frac{z_0}{d}\omega_0 \simeq \begin{cases} v_{x0}\omega_\perp & \text{for } Qt = 2n\pi, \\ \left(1 - \frac{2\omega_\parallel^2}{Q^2}\right) v_{x0}\omega_\perp & \text{for } Qt = 2(n+1)\pi. \end{cases} \tag{28}$$

Therefore, the electron will de-trap from wave potential at larger velocity v_{x0}, when the stronger longitudinal magnetic field B_y is superposed in the current sheet. This conclusion has been further identified by test particle simulation, as shown in Fig. 9.

Another limitation of the electron surfing acceleration in current sheet is caused by the electron escapes from the z

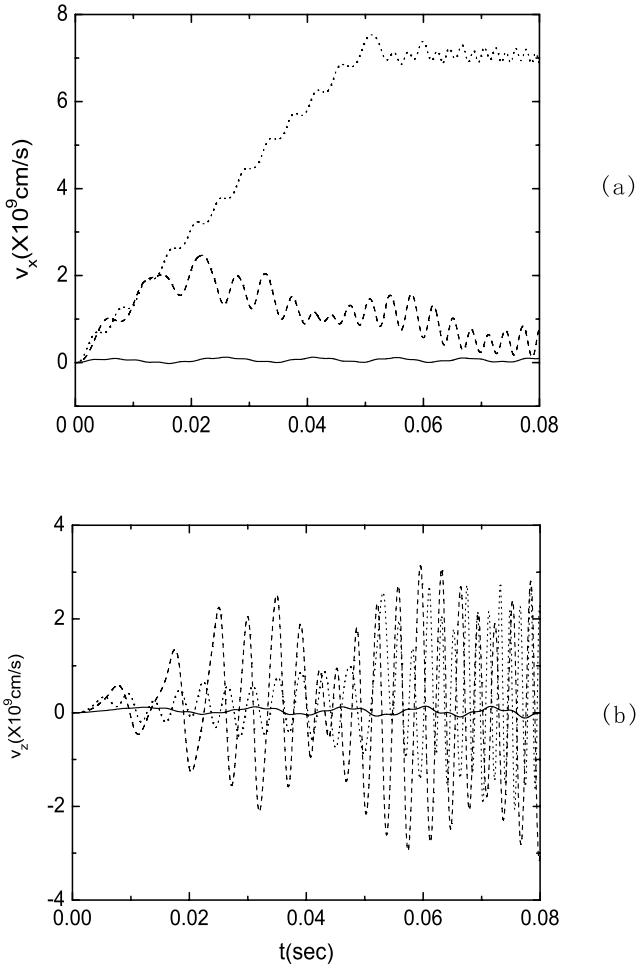

Fig. 8 The time evolution of electron velocity trajectory by test particle simulation for $K > 0$ with different E_0 and same B_y. Other parameters are the same as that in Fig. 2. In the figure, the solid, dash and dot lines represent that case for $E_0 = 10$, 40, 80 mV/m, respectively: **a** v_x, **b** v_z

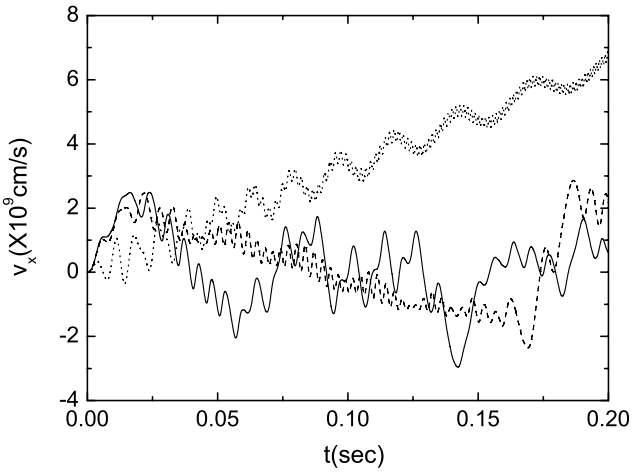

Fig. 9 The time evolution of electron velocity trajectory v_x by test particle simulation for $K > 0$ with same $E_0 = 40$ mV/m and different B_y. Other parameters are the same as that in Fig. 2. In the figure, the solid, dash and dot lines represent that case for $B_y = (-5.0, -1.0, -0.50) \times 10^{-5}$ G, respectively

boundary of current sheet. It was discussed in above section that the electron could be rapidly accelerated in the z direction for the case of $K < 0$, it makes electron escapes rapidly from z boundary of current sheet. Otherwise, the electron should escape from z boundary of current sheet yet, when $|z_0 - z_0(0)| \geq d$, even if the electron is mainly accelerated in the x direction for the case of $K > 0$. We obtain another acceleration limitation time of electron escaping t_e in the zeroth order approximation (15) as

$$t_e \leq \frac{dQ^2}{\omega_\perp \omega_\parallel v_p}. \tag{29}$$

Insertion of (27) into v_{x0} of expression (16). We find the limited electron velocity v_{xM} in the x direction may be written as

$$v_{xM} \leq \frac{B_0}{B_y} v_p. \tag{30}$$

Third limitation of electron surfing acceleration in current sheet is the spatial size of the acceleration region. The maximum attainable energy may be expressed as

$$E_{\max} \leq \frac{ev_p}{c} B_z L \tag{31}$$

where L is the spatial size of acceleration region in the x direction of current sheet.

The electron surfing acceleration in magnetic reconnection region has also been investigated by Hoshino (2005) and Fu et al. (2006). He think that a polarization electric field near X-type magnetic reconnection are induced. The electrons are trapped by the potential of the polarization field. These trapped electrons can be accelerated in the perpendicular direction to current sheet by surfing acceleration. However, we can find that the direction of electrostatic field and acceleration velocity for two kinds of surfing acceleration suggested by Hoshino (2005) and Fu et al. (2006) and discussed in this paper are quite different.

It was assumed in the above simplified theoretical model that the amplitude of electrostatic waves and perpendicular magnetic field B_z are homogeneous in the current sheet, and they are invariant in time. The shear magnetic field B_x in the current sheet is also independent from time. In fact, these assumption are inconsistent with the particle simulation results of the magnetic reconnection. Horiuchi and Sato (1999) found from three dimensional particle simulation of collisionless reconnection that the lower hybrid drift electrostatic waves will evolve after the linear growth stage. Drake et al. (2003) found that the Langmuir waves excited by Buneman instability at the central current sheet in the linear stage, and then this instability evolve into a nonlinear electron hole. Imada et al. (2005), Drake et al. (2006)

showed that the electron acceleration in the magnetic reconnection region occurs not only around the X-point, but also in more wider region. These results show that electron surfing acceleration in the current sheet may be very complicated. Meanwhile, other electron acceleration mechanisms may play an important role in the different evolution time of reconnection (Hoshino 2005). It is required to further study the influence of these factors on the surfing acceleration in current sheet.

Here, we summarize the conclusion based on the above calculation:

(1) The electrons can be fast accelerated in the current sheet plane (x, z) by $\frac{ev_p}{c} \times B_z$ force, when they are trapped in the potential of electrostatic waves and an uniform perpendicular transverse magnetic field B_z is superposed. This surfing acceleration process is only effective when the criterion of $K = \omega_{\parallel}^2 - \frac{v_p}{d}\omega_0 > 0$ holds. Otherwise, the acceleration electron will escape from the current sheet quickly for the case of $K < 0$.

(2) The approximation condition $|V_Y| \ll v_p$ of analytical solution is usually satisfied in the early stage of time evolution. The surfing acceleration velocity of electron v_x in the current sheet is often much larger than v_z for the case of $K > 0$. In the case of $B_y \to 0$, the maximum velocity of electron by surfing acceleration in current sheet is about the same as the electric drift velocity, which is proportional to the amplitude of electrostatic wave E_0. The acceleration process will continue until the electron de-traps from potential of electrostatic wave at the turning point, or escapes from the x and z boundaries of current sheet.

(3) Superposed a longitudinal magnetic field B_y along the propagating direction of wave may be favorable for the electron surfing acceleration in the current sheet.

Acknowledgements The authors gratefully acknowledge support for this work from National Foundation of Sciences in China (NSFC) under Grants (No. 10425312 and No. 40674093). We would like to thank the reviewer for his useful comments.

References

Bale, S.D., Mozer, F.S., Phan, T.: Geophys. Res. Lett. **29** (2002). doi:10.1029/2002GL016113

Birdsall, C.K., Langdonm, A.B. (eds.): Plasma Physics via Computer Simulation. McGraw–Hill, New York (1985)

Browning, P.K., Vekstein, G.E.: J. Geophys. Res. **106**, 18677 (2001)

Dawson, J.M., Decyk, V.K., Huff, R.W., Jechart, I., Katsouleas, T., Leboeuf, J.N., Lembege, B., Martinez, R.M., Ohsawa, Y., Ratliff, S.T.: Phys. Rev. Lett. **50**, 1455 (1983)

Drake, J.K., Swisdak, M., Cattell, C., Shay, M.A., Rogers, N.B., Zeiler, A.: Science **299**, 873 (2003)

Drake, J.K., Swisdak, M., Che, H., Shay, M.A.: Nature **443**, 553 (2006)

Farrell, W.M., Desch, M.D., Kaiser, M.L., Geotz, K.: Geophys. Res. Lett. **29** (2002). doi:10.1029/2002GL014662

Fu, X.M., Lu, Q.M., Wang, S.: Phys. Plasmas **13**, 012309 (2006)

Himilton, B., McClements, K.G., Fletcher, L., Thyagaraja, A.: Astrophys. J. **625**, 496 (2003)

Horiuchi, R., Sato, T.: Phys. Plasmas **6**, 4565 (1999)

Hoshino, M.: J. Geophys. Res. **110**, A10215 (2005). doi:10.1029/2005JA011229

Imada, S., Hoshino, M., Mukai, T.: Geophys. Res. Lett. **32**, L09101 (2005). doi:10.1029/2005GL022594

Katsouleas, T., Dawson, J.M.: Phys. Rev. Lett. **51**, 392 (1983)

Labelle, J.A., Treumann, R.: Space Sci. Rev. **47**, 175 (1988)

Litvinenko, Y.E., Somov, B.V.: Solar Phys. **146**, 127 (1993)

Øieroset, M., Lin, R.P., Plan, T.D., Larson, D.E., Sale, S.D.: Phys. Rev. Lett. **89**, 195001 (2002)

Pritchett, P.L.: J. Geophys. Res. **111**, A10212 (2006). doi:10.1029/2006JA011793

Speiser, T.W.: J. Geophys. Res. **70**, 4219 (1965)

Sugihara, R., Takeuchi, S., Sakai, K., Matsumoto, M.: Phys. Rev. Lett. **52**, 1500 (1984)

Zhong, D.K., Wei, F.S., Feng, X.S., Yang, F.: Chin. Phys. Lett. **22**, 3225 (2005)

Zhu, Z.W., Parks, G.: J. Geophys. Res. **98**, 7603 (1993)